JOURNAL OF COMPUTATIONAL PHYSICS 59, 468–483 (1985)

Reconstruction of the Time-Dependent Monoenergetic Neutron Flux from Moments

B. D. GANAPOL

Department of Nuclear and Energy Engineering, University of Arizona, Tucson, Arizona 85021

Received June 22, 1984; revised October 16, 1984

The solution to the monoenergetic time-dependent neutron transport equation in infinite spherical geometry with isotropic scattering is reconstructed from moments. By application of the transformation between spherical and cylindrical geometry, the corresponding solutions is obtained directly. In addition, the form of the solution allows generalization to the anisotropic scattering case.

1. INTRODUCTION

Some time ago, an article appeared in this Journal which was concerned with the numerical solution of the monoenergetic time-dependent neutral particle transport equation in infinite spherical geometry [1]. The approach taken was the rather awkward procedure of considering the Laplace transform as an integral equation and solving the equation using known transform data obtained from the corresponding stationary solution. The temporal variable was partitioned into early and late regimes and an involved least squares fitting procedure was employed to obtain the desired numerical solution. This ad hoc procedure suffered from several serious faults. In particular, the process was not automated and required manual intervention to provide the necessary feedback in order to converge to a desired accuracy. In addition, the procedure had to be applied separately at each spatial position and had to be completely redone for a change in scattering cross section. A comparison with solutions found by discrete ordinates and Monte Carlo methods indicated a significant discrepancy; and based on an integral measure, the authors concluded that their solution was the most accurate.

A transform solution expressed as a polynomial expansion in the spatial variable was also discussed in Ref. [1] but no results of the inversion were presented. In the discussion, it was indicated that the polynomial expansion did not converge sufficiently rapidly enough for the intended inversion and in some instances (large values of the transform variable) failed to converge as a result of round off error accumulation. For this reason, the moment reconstruction technique was considered to be limited relative to the discrete ordinates and Monte Carlo methods for generating the time-dependent flux.

0021-9991/85 $3.00

It will be the purpose of this presentation to demonstrate that the method of moments, if properly applied, is a valid computational technique and can provide an accurate solution for all time; the method can be easily modified to include cylindrical geometry and anisotropic scattering. The main feature of the polynomial expansion is the incorporation of the wavefront, associated with the neutron motion resulting from a spatially localized pulsed source, directly into the expansion. In addition, the Laplace transform inversion of the required moments will be performed analytically thus providing a convenient expression to be evaluated numerically. The numerical solution obtained by the expansion is then compared to that obtained via the multiple collision approach indicating at least four-place accuracy at any position for times after the passage of the wavefront. The numerical evaluation will also be compared to the fitting procedure described above [1], thus providing a measure of its absolute accuracy.

2. Plane–Point Transformation

In one-dimensional plane geometry, the most fundamental monoenergetic time-dependent neutron transport problem is described by [2]

$$\left[\frac{\partial}{\partial t}+\mu\frac{\partial}{\partial x}+1\right]\phi^{\mathrm{pl}}(x,\mu,t;c)=\frac{c}{2}\int_{-1}^{1}d\mu'\,\phi^{\mathrm{pl}}(x,\mu',t;c)+\frac{1}{2}\delta(x)\,\delta(t)$$

$$\phi^{\mathrm{pl}}(x,\mu,t;c)=0,\qquad t<0 \tag{1}$$

$$\lim_{|x|\to\infty}\phi^{\mathrm{pl}}(x,\mu,t;c)=0.$$

Isotropic scattering is assumed and a source at $x=0$ emits neutrons isotropically at time $t=0$. The time t and position x are measured in terms of mean free time and mean free path, respectively. c is the number of secondary neutrons resulting from a collision. In the following, only the case $c=1$ will be considered since [2]

$$\phi(x,\mu,t;c)=ce^{-(1-c)t}\phi(cx,\mu,ct;1)$$

and the dependence on c will be suppressed. From the well-known plane–point transformation, which holds even for anisotropic scattering [2], the scalar flux,

$$\phi(r,t)=\int_{-1}^{1}d\mu\,\phi(r,\mu,t),$$

in spherical geometry is related to scalar flux in plane geometry by

$$\phi^{\mathrm{sp}}(r,t)=-\frac{1}{2\pi r}\frac{\partial\phi^{\mathrm{pl}}(r,t)}{\partial r}. \tag{2}$$

Thus if an analytical expression is found for $\phi^{\text{pl}}(r, t)$, then the flux in infinite spherical geometry for the corresponding isotropic source at $r=0$ is obtained by differentiation.

Because of the spatially localized nature of the source, the solution in plane (spherical and cylindrical) geometry is known to exhibit a wavefront at $x=t$ resulting from a fixed finite neutron speed ($v=1$ in this case) [3]. Thus, a natural polynomial expansion for the scalar flux in plane geometry is

$$\phi^{\text{pl}}(x, t)=\sum_{k=0}^{\infty} \frac{2k+1}{2} f_k(t)\, P_k(\eta)\, \theta(1-|\eta|) \tag{3}$$

where

$$\eta \equiv x/t$$

and P_k is the k^{th} Legendre polynomial with θ being the Heaviside unit step function. The moments f_k are determined from the orthogonality of the Legendre polynomials

$$f_k(t) \equiv \int_{-1}^{1} d\eta'\, P_k(\eta')\, \phi^{\text{pl}}(x', t). \tag{4}$$

In this way, neutrons are constrained to always remain behind the wavefront, thus eliminating the propagation of numerical error ahead of the front. Now substituting Eq. (3) into (2) yields

$$\phi^{\text{sp}}(r, t)=\phi_0(r, t)+\frac{1}{2\pi r t(1-\eta^2)} \times \sum_{k=1}^{\infty}\left(\frac{2k+1}{2}\right) k f_k(t)[\eta P_k(\eta)-P_{k-1}(\eta)]\, \theta(1-\eta) \tag{5}$$

where the expression

$$\frac{d}{d\eta} P_k(\eta)=\frac{k}{1-\eta^2}\,[P_{k-1}(\eta)-\eta P_k(\eta)]$$

has been used [4]. ϕ_0 is the uncollided contribution given by

$$\phi_0(r, t)=\frac{e^{-t}}{4\pi r t^2}\,\delta(1-\eta);$$

and the second term represents the scattered contribution. Because of the symmetry of ϕ^{pl}

$$f_{2k+1}(t)=0$$

and the summation in Eqs. (3) and (5) are over even values of k only. In the next section, the Legendre moments f_k will be determined in terms of spatial moments to be obtained explicitly.

3. Determination of f_k

By expressing P_k in its polynomial representation, Eq. (4) becomes

$$f_k(t) = \sum_{j=0}^{[k/2]} a_{k,j} M_{k-2j}(t)/t^{k-2j+1} \tag{6}$$

with

$$a_{k,j} \equiv \frac{(-1)^j(2k-2j)!}{2^j j!(k-j)!(k-2j)!}$$

and where the spatial moments are defined by

$$M_k(t) = \int_{-\infty}^{\infty} dx\, x^k \phi^{\mathrm{pl}}(x, t). \tag{7}$$

The spatial moments can be found analytically by first multiplying Eq. (1) by x^k and integrating over x to give

$$\begin{gathered} \frac{\partial}{\partial t} M_k(\mu, t) - k\mu M_{k-1}(\mu, t) + M_k(\mu, t) = \frac{1}{2} M_k(t) + \frac{1}{2} \delta_{k,0}\, \delta(t) \\ M_k(\mu, 0) = 0 \end{gathered} \tag{8}$$

where

$$M_k(\mu, t) \equiv \int_{-\infty}^{\infty} dx\, x^k\, \phi^{\mathrm{pl}}(x, \mu, t).$$

Then by making the substitution

$$M_k(\mu, t) = e^{-t} \hat{M}_k(\mu, t) \tag{9}$$

and taking a Laplace transform of Eq. (8), we find

$$s\bar{M}_k(\mu, s) - k\mu \bar{M}_{k-1}(\mu, s) = \tfrac{1}{2}\bar{M}_k(s) + \tfrac{1}{2}\delta_{k,0} \tag{10}$$

with

$$\bar{M}_k(\mu, s) \equiv \int_0^{\infty} dt\, e^{-st} \hat{M}_k(\mu, t).$$

Finally, Eq. (10) is solved analytically as a finite difference equation and the result inverted to give [5]

$$M_{2k}(t) = (2k)(2k-1) \sum_{r=0}^{k-1} \frac{\alpha_r^k}{(r+1)!} I_{r+1,2k-2}(t) \tag{11a}$$

with

$$I_{r,q}(t) \equiv \int_0^t dt'\, e^{-t'}(t-t')^r t'^q \tag{11b}$$

and

$$\begin{aligned} \alpha_0^k &= \frac{1}{2k+1} \\ \alpha_r^k &= \sum_{j=r}^{k-1} \frac{\alpha_{r-1}^{j'}}{2(k-j')+1}, \qquad 1 \leqslant r \leqslant k-1. \end{aligned} \tag{11c}$$

$I_{r,k}$ can also be expressed in a closed form; however, for best numerical results the representation in terms of incomplete γ functions is preferred

$$I_{t,q}(t) = t^{r+1} \sum_{l=0}^{r} \frac{(-1)^l r!}{l!(r-l)! t^l} \gamma(k+l+1, t) \tag{12}$$

where

$$\gamma(k, t) = \int_0^t dt'\, t'^{k-1} e^{-t'}.$$

The final result is obtained from Eqs. (5), (6), (11), and (12).

4. Cylindrical Geometry

Once the flux in spherical geometry is obtained, the transformation

$$\phi^{cy}(r, t) = 2 \int_0^\infty dz\, \phi^{sp}(\sqrt{r^2+z^2}, t) \tag{13}$$

will give the scalar flux in cylindrical geometry or

$$\phi^{cy}(r, t) = \frac{e^{-t}}{2\pi t^2 \sqrt{1-\eta^2}} - \frac{1}{\pi t} \sum_{k=2}^{\infty} \frac{2k+1}{2} f_k(t)\, J_k(\eta) \tag{14}$$

with

$$J_k(\eta) \equiv \int_\eta^1 d\eta' \frac{P'_{k(\eta')}}{\sqrt{\eta'^2 - \eta^2}}. \tag{15}$$

The integral defined in Eq. (15) can be evaluated in closed form for k an even integer

$$J_k(\eta) = \sum_{j=0}^{[k/2]-1} b_{k,j} q_{k-2j-1}(\eta) \tag{16}$$

where

$$b_{k,j} = (k-2j)\, a_{k,j}$$

and where q_k can be evaluated recursively

$$\begin{aligned} q_1(\eta) &= \sqrt{1-\eta^2} \\ q_k(\eta) &= \frac{1}{k}\sqrt{1-\eta^2} + \frac{k-1}{k}\eta^2 q_{k-2}(\eta) \end{aligned} \tag{17}$$

to complete the determination. $J_k(\eta)$ can also be shown to be proportional to a polynomial in η^2.

5. Anisotropic Scattering

For general anisotropic scattering, Eq. (1) becomes

$$\left[\frac{\partial}{\partial t} + \mu\frac{\partial}{\partial x} + 1\right]\phi^{\text{pl}}(x, \mu, t; c) = c\sum_{l=0}^{L}\frac{2l+1}{2}\omega_l P_l(\mu)\int_{-1}^{1} d\mu'\, P_l(\mu') \times \phi^{\text{pl}}(x, \mu', t; c) + \frac{1}{2}\delta(x)\,\delta(t), \tag{18}$$

where the anisotropic scattering kernel has been expanded in terms of Legendre polynomials and ω_0 is taken as unity. The geometry transfer formulas Eqs. (2) and (13) are valid for this case. Therefore, all results except those for the determination of $M_k(t)$ are applicable for anisotropic scattering. For this case, no convenient analytical expression for $M_k(t)$ seems to exist. All is not lost, however, since one can show that [5]

$$M_k(t) = e^{-t} t^k \sum_{n=0}^{\infty}\frac{(ct)^n}{n!}\beta(n, k, 0) \tag{19a}$$

with $\beta(n, k, l)$ given recursively by

$$\beta(0, k, l) = 2^{m-k} \frac{k!}{(m-l)!(2m+1)!!}, \qquad 2m = l + k$$

$$(k+n)\,\beta(n, k, l) = n\omega_l \beta(n-1, k, l) + \frac{k}{2l+1}\,[l\beta(n, k-1, l-1) + (l+1)\,\beta(n, k-1, l+1)]. \tag{19b}$$

Equations (19) result from application of the multiple collision formalism to Eq. (18) and noting that the solution rigorously satisfies the expansion in collided fluxes

$$\phi(x, \mu, t) = \frac{e^{-t}}{t} \sum_{n=0}^{\infty} \frac{(ct)^n}{n!} F_n(\mu, \eta)\,\theta(1 - |\eta|). \tag{20}$$

6. Results

The first part of this section is devoted to establishing the credibility of the proposed expansion. The evaluation of the infinite series in the flux representations given by Eqs. (5) and (14) is considered to be "numerically" converged when three consecutive terms produce a relative error of less than 5×10^{-5}. Also since the moment reconstruction technique is known to be an ill-condition process in general, all calculations were performed in CDC double precision arithmetic.

The first comparison is with an independent determination of ϕ^{sp} using the multiple collision method [3]. Table I shows the spherical scalar flux for six positions

TABLE I

SPHERICAL GEOMETRY C= 1.0000E+00 SCALAR FLUX - ISOTROPIC SOURCE

T/X	1.0000E+00	2.0000E+00	3.0000E+00	4.0000E+00	5.0000E+00	6.0000E+00
1.0000E+00*	∞	0.	0.	0.	0.	0.
3.0000E+00*	2.2002E-02	1.0187E-02	∞	0.	0.	0.
5.0000E+00*	1.0350E-02	6.5738E-03	2.9564E-03	8.5546E-04	∞	0.
7.0000E+00*	6.2716E-03	4.5417E-03	2.6144E-03	1.1654E-03	3.8287E-04	8.3429E-05
9.0000E+00*	4.3089E-03	3.3538E-03	2.1944E-03	1.1937E-03	5.3016E-04	1.8655E-04
1.1000E+01*	3.1916E-03	2.6004E-03	1.8417E-03	1.1274E-03	5.9123E-04	2.6210E-04
1.3000E+01*	2.4854E-03	2.0900E-03	1.5625E-03	1.0350E-03	6.0442E-04	3.0893E-04
1.5000E+01*	2.0059E-03	1.7263E-03	1.3423E-03	9.4107E-04	5.9294E-04	3.3430E-04
1.7000E+01*	1.6829E-03	1.4566E-03	1.1670E-03	8.5397E-04	5.6950E-04	3.4514E-04
1.9000E+01*	1.4076E-03	1.2503E-03	1.0256E-03	7.7604E-04	5.4089E-04	3.4656E-04
2.1000E+01*	1.2115E-03	1.0884E-03	9.0986E-04	7.0730E-04	5.1071E-04	3.4204E-04
2.3000E+01*	1.0570E-03	9.5851E-04	8.1396E-04	6.4694E-04	4.8086E-04	3.3389E-04
2.5000E+01*	9.3283E-04	8.5252E-04	7.3353E-04	5.9394E-04	4.5229E-04	3.2363E-04
2.7000E+01*	8.3117E-04	7.6470E-04	6.6536E-04	5.4732E-04	4.2542E-04	3.1225E-04
2.9000E+01*	7.4672E-04	6.9096E-04	6.0702E-04	5.0615E-04	4.0042E-04	3.0038E-04
3.1000E+01*	6.7585E-04	6.2834E-04	5.5666E-04	4.6967E-04	3.7728E-04	2.8843E-04
3.3000E+01*	6.1519E-04	5.7464E-04	5.1284E-04	4.3720E-04	3.5595E-04	2.7666E-04
3.5000E+01*	5.6323E-04	5.2816E-04	4.7444E-04	4.0819E-04	3.3630E-04	2.6523E-04
3.7000E+01*	5.1820E-04	4.8762E-04	4.4058E-04	3.8218E-04	3.1820E-04	2.5424E-04
3.9000E+01*	4.7886E-04	4.5201E-04	4.1054E-04	3.5873E-04	3.0152E-04	2.4374E-04
4.1000E+01*	4.4426E-04	4.2053E-04	3.8375E-04	3.3754E-04	2.8615E-04	2.3375E-04
4.3000E+01*	4.1363E-04	3.9254E-04	3.5974E-04	3.1833E-04	2.7195E-04	2.2427E-04
4.5000E+01*	3.8637E-04	3.6752E-04	3.3812E-04	3.0083E-04	2.5882E-04	2.1530E-04

1(1)6 from a source at $r=0$ and for $c=1$. A comparison was made with Table II of Ref. [3], where the values are reported to four significant figures. The digits that are underlined in the table are in disagreement by one unit in the last place. Except for positions near the wavefront, the agreement is excellent and within the stated accuracy. The inaccuracy at the wavefront is expected since, as a rule, polynomial approximations do not simulate discontinuities to a high degree of accuracy. As a second confirmation, the corresponding cylindrical source problem was compared to the multiple collision results which are reported to three-place accuracy [3]. The results, shown in Table II, are again in excellent agreement except near the wavefront. The slight reduction in the agreement for the cylindrical source relative to the spherical source is, in part, a result of the reduced accuracy of the multiple collision calculation. In addition, since the evaluation in cylindrical geometry involves an added recursion relation and sum, Eqs. (16) and (17), the potential for round off error accumulation is greater.

A second general comparison was made with the standard diffusion solution in spherical geometry [3]

$$\phi_D^{sp}(r,t)=\frac{e^{-r^2/4Dt}}{(4\pi Dt)^{3/2}}, \qquad D=1/3c$$

with the relative error

$$\varepsilon=|\phi^{sp}-\phi_D^{sp}|/\phi^{sp}$$

given in Tables III and IV for $c=1$ and 0.3, respectively. For both values of c, the transport theory solution approaches diffusion theory with increasing time as

TABLE II

CYLINDRICAL GEOMETRY C= 1.0000E+00 SCALAR FLUX - ISOTROPIC SOURCE

T/X	1.0000E+00	2.0000E+00	3.0000E+00	4.0000E+00	5.0000E+00	6.0000E+00
1.0000E+00*	∞	0.	0.	0.	0.	0.
3.0000E+00*	7.4301E-02	3.1994E-02	∞	0.	0.	0.
5.0000E+00*	4.6005E-02	2.8590E-02	1.2309E-02	3.2633E-03	∞	0.
7.0000E+00*	3.3257E-02	2.3833E-02	1.3461E-02	5.8196E-03	1.8194E-03	3.6204E-04
9.0000E+00*	2.6028E-02	2.0135E-02	1.3033E-02	6.9756E-03	3.0263E-03	1.0294E-03
1.1000E+01*	2.1376E-02	1.7346E-02	1.2201E-02	7.3928E-03	3.8227E-03	1.6628E-03
1.3000E+01*	1.8133E-02	1.5205E-02	1.1312E-02	7.4409E-03	4.3042E-03	2.1729E-03
1.5000E+01*	1.5744E-02	1.3521E-02	1.0476E-02	7.3064E-03	4.5721E-03	2.5552E-03
1.7000E+01*	1.3911E-02	1.2165E-02	9.7197E-03	7.0842E-03	4.6998E-03	2.8296E-03
1.9000E+01*	1.2460E-02	1.1053E-02	9.0465E-03	6.8239E-03	4.7367E-03	3.0193E-03
2.1000E+01*	1.1282E-02	1.0125E-02	8.4493E-03	6.5518E-03	4.7150E-03	3.1447E-03
2.3000E+01*	1.0308E-02	9.3383E-03	7.9191E-03	6.2809E-03	4.6558E-03	3.2219E-03
2.5000E+01*	9.4893E-03	8.6659E-03	7.4470E-03	6.0193E-03	4.5731E-03	3.2630E-03
2.7000E+01*	8.7907E-03	8.0825E-03	7.0250E-03	5.7700E-03	4.4761E-03	3.2775E-03
2.9000E+01*	8.1878E-03	7.5723E-03	6.6462E-03	5.5346E-03	4.3711E-03	3.2722E-03
3.1000E+01*	7.6623E-03	7.1224E-03	6.3047E-03	5.3135E-03	4.2620E-03	3.2523E-03
3.3000E+01*	7.2002E-03	6.7228E-03	5.9955E-03	5.1062E-03	4.1518E-03	3.2218E-03
3.5000E+01*	6.7907E-03	6.3654E-03	5.7144E-03	4.9122E-03	4.0423E-03	3.1836E-03
3.7000E+01*	6.4252E-03	6.0441E-03	5.4579E-03	4.7306E-03	3.9347E-03	3.1399E-03
3.9000E+01*	6.0971E-03	5.7535E-03	5.2230E-03	4.5606E-03	3.8298E-03	3.0924E-03
4.1000E+01*	5.8008E-03	5.4895E-03	5.0071E-03	4.4014E-03	3.7281E-03	3.0423E-03
4.3000E+01*	5.5320E-03	5.2487E-03	4.8080E-03	4.2520E-03	3.6299E-03	2.9907E-03
4.5000E+01*	5.2870E-03	5.0280E-03	4.6240E-03	4.1119E-03	3.5352E-03	2.9382E-03

TABLE III

SPHERICAL GEOMETRY C= 1.0000E+00 SCALAR FLUX - ISOTROPIC SOURCE

DIFFUSION COMPARISON

T/X	1.0000E+00	2.0000E+00	3.0000E+00	4.0000E+00	5.0000E+00	6.0000E+00
1.0000E+00*	∞	0.	0.	0.	0.	0.
5.0000E+00*	1.3236E-01	1.2900E-01	8.5162E-02	1.0638E-01	∞	0.
9.0000E+00*	7.7543E-02	7.7011E-02	7.0028E-02	4.6015E-02	1.4649E-02	1.5300E-01
1.3000E+01*	5.4851E-02	5.4681E-02	5.2385E-02	4.4753E-02	2.6747E-02	9.4722E-03
1.7000E+01*	4.2435E-02	4.2361E-02	4.1336E-02	3.7964E-02	3.0167E-02	1.4998E-02
2.1000E+01*	3.4603E-02	3.4564E-02	3.4021E-02	3.2240E-02	2.8155E-02	2.0317E-02
2.5000E+01*	2.9212E-02	2.9189E-02	2.8869E-02	2.7813E-02	2.5407E-02	2.0817E-02
2.9000E+01*	2.5274E-02	2.5260E-02	2.5055E-02	2.4379E-02	2.2842E-02	1.9922E-02
3.3000E+01*	2.2271E-02	2.2262E-02	2.2123E-02	2.1665E-02	2.0623E-02	1.8650E-02
3.7000E+01*	1.9907E-02	1.9900E-02	1.9801E-02	1.9502E-02	1.8739E-02	1.7342E-02
4.1000E+01*	1.7996E-02	1.7990E-02	1.7918E-02	1.7687E-02	1.7138E-02	1.6113E-02
4.5000E+01*	1.6420E-02	1.6415E-02	1.6361E-02	1.6186E-02	1.5773E-02	1.4997E-02
4.9000E+01*	1.5096E-02	1.5094E-02	1.5052E-02	1.4917E-02	1.4588E-02	1.3997E-02
5.3000E+01*	1.3971E-02	1.3969E-02	1.3936E-02	1.3829E-02	1.3581E-02	1.3104E-02
5.7000E+01*	1.3002E-02	1.2999E-02	1.2974E-02	1.2888E-02	1.2711E-02	1.2305E-02
6.1000E+01*	1.2156E-02	1.2156E-02	1.2136E-02	1.2065E-02	1.1919E-02	1.1593E-02
6.5000E+01*	1.1416E-02	1.1416E-02	1.1397E-02	1.1341E-02	1.1218E-02	1.0951E-02
6.9000E+01*	1.0761E-02	1.0761E-02	1.0745E-02	1.0698E-02	1.0602E-02	1.0376E-02
7.3000E+01*	1.0174E-02	1.0175E-02	1.0164E-02	1.0123E-02	1.0040E-02	9.8579E-03
7.7000E+01*	9.6512E-03	9.6516E-03	9.6394E-03	9.6051E-03	9.5338E-03	9.4429E-03

TABLE IV

SPHERICAL GEOMETRY C= 3.0000E-01 SCALAR FLUX - ISOTROPIC SOURCE

DIFFUSION COMPARISON

T/X	1.0000E+00	2.0000E+00	3.0000E+00	4.0000E+00	5.0000E+00	6.0000E+00
1.0000E+00*	∞	0.	0.	0.	0.	0.
5.0000E+00*	3.2303E-01	3.3667E-01	3.5593E-01	3.8003E-01	∞	0.
9.0000E+00*	2.1511E-01	2.1838E-01	2.2281E-01	2.2621E-01	2.2575E-01	2.1687E-01
1.3000E+01*	1.6090E-01	1.6218E-01	1.6385E-01	1.6525E-01	1.6509E-01	1.6198E-01
1.7000E+01*	1.2835E-01	1.2897E-01	1.2978E-01	1.3046E-01	1.3045E-01	1.2906E-01
2.1000E+01*	1.0664E-01	1.0700E-01	1.0746E-01	1.0784E-01	1.0785E-01	1.0712E-01
2.5000E+01*	9.1193E-02	9.1411E-02	9.1697E-02	9.1932E-02	9.1945E-02	9.1517E-02
2.9000E+01*	7.9636E-02	7.9779E-02	7.9967E-02	8.0122E-02	8.0135E-02	7.9862E-02
3.3000E+01*	7.0668E-02	7.0767E-02	7.0897E-02	7.1005E-02	7.1016E-02	7.0832E-02
3.7000E+01*	6.3510E-02	6.3582E-02	6.3675E-02	6.3753E-02	6.3762E-02	6.3633E-02
4.1000E+01*	5.7666E-02	5.7719E-02	5.7789E-02	5.7847E-02	5.7854E-02	5.7760E-02
4.5000E+01*	5.2805E-02	5.2845E-02	5.2898E-02	5.2943E-02	5.2949E-02	5.2878E-02
4.9000E+01*	4.8698E-02	4.8730E-02	4.8771E-02	4.8806E-02	4.8811E-02	4.8756E-02
5.3000E+01*	4.5183E-02	4.5208E-02	4.5241E-02	4.5269E-02	4.5273E-02	4.5230E-02
5.7000E+01*	4.2141E-02	4.2161E-02	4.2188E-02	4.2210E-02	4.2214E-02	4.2179E-02
6.1000E+01*	3.9482E-02	3.9498E-02	3.9520E-02	3.9539E-02	3.9542E-02	3.9514E-02
6.5000E+01*	3.7138E-02	3.7152E-02	3.7170E-02	3.7185E-02	3.7188E-02	3.7165E-02
6.9000E+01*	3.5057E-02	3.5069E-02	3.5084E-02	3.5097E-02	3.5099E-02	3.5080E-02
7.3000E+01*	3.3196E-02	3.3206E-02	3.3219E-02	3.3230E-02	3.3232E-02	3.3216E-02
7.7000E+01*	3.1523E-02	3.1532E-02	3.1543E-02	3.1552E-02	3.1554E-02	3.1540E-02

required by the Boltzmann H theorem. Also, as expected, the transport theory solution approaches diffusion theory more rapidly for a medium with reduced absorption (larger c).

It is also instructive to compare the moment reconstructions with the more accurate transport (pole) approximation derived by Boffi [6] (see Appendix). A dramatic improvement over standard diffusion theory is seen from the relative error shown in Tables V and VI. In effect, the pole approximation is almost as accurate as the transport solution for all but early times ($t < 9$).

The final comparison is with the fitted solution obtained in Ref. [1]. The relative error between the two solutions is presented in Fig. 1. with the fitting parameters taken from Table IV of Ref. [1]. In general, the agreement is rather poor and exhibits the same behavior as found in Ref. [1] when the fitted solution was compared to time-dependent ANISN (TDA) results. The large discrepancy at short times is apparently due to a conceptual error made in Ref. [1] regarding the scattered flux contribution. It was assumed that the scattered flux was zero when the wavefront first reaches a given position ($\eta = 1$). However, as shown in Ref. [3], a logarithmic singularity resulting from the divergence associated with spherical geometry exists at $\eta = 1$. Thus, the fitted flux was incorrectly forced to zero at the wavefront producing a large discrepancy when compared to a more exact determination. The error and eventual divergence at long times is more serious. It is clear from the comparison that the fitted solution does not approach diffusion theory as time increases casting serious doubt on the accuracy of this procedure.

TABLE V

SPHERICAL GEOMETRY C= 3.0000E-01 SCALAR FLUX - ISOTROPIC SOURCE

POLE COMPARISON

T/X	1.0000E+00	2.0000E+00	3.0000E+00	4.0000E+00	5.0000E+00	6.0000E+00
1.0000E+00*	∞	0.	0.	0.	0.	0.
3.0000E+00*	9.9743E-02	5.7911E-02	∞	0.	0.	0.
5.0000E+00*	2.0218E-02	1.2161E-02	8.3666E-03	2.7684E-02	∞	0.
7.0000E+00*	5.8171E-03	3.5157E-03	1.6974E-03	2.4668E-03	8.8808E-03	2.9998E-02
9.0000E+00*	2.1355E-03	1.2301E-03	5.4336E-04	3.9160E-04	1.4980E-03	3.9958E-03
1.1000E+01*	8.8123E-04	5.4792E-04	2.2784E-04	4.6828E-05	3.8193E-04	1.0292E-03
1.3000E+01*	4.3875E-04	2.4388E-04	4.4065E-05	3.3424E-05	8.4119E-05	3.7536E-04
1.5000E+01*	2.0342E-04	1.4075E-04	6.5025E-05	2.3513E-07	5.1710E-05	1.4645E-04
1.7000E+01*	1.5509E-04	8.6761E-05	1.9691E-05	6.5899E-06	2.0081E-05	8.1089E-05
1.9000E+01*	9.3608E-05	5.5628E-05	1.5209E-05	4.0870E-06	6.8016E-06	4.3811E-05
2.1000E+01*	4.5778E-05	3.1373E-05	1.1921E-05	2.4855E-06	2.3677E-06	2.4144E-05
2.3000E+01*	3.1688E-05	2.1468E-05	9.4135E-06	6.5619E-07	3.7490E-06	1.3708E-05
2.5000E+01*	2.2640E-05	1.5327E-05	6.7818E-06	1.2194E-06	9.1096E-07	9.1520E-06
2.7000E+01*	1.8406E-05	1.2334E-05	5.1035E-06	1.0325E-06	8.7779E-07	6.2546E-06
2.9000E+01*	1.3358E-05	9.1223E-06	4.1316E-06	9.1157E-07	1.0544E-06	4.3640E-06
3.1000E+01*	9.9235E-06	6.8827E-06	3.2725E-06	7.5414E-07	8.2197E-07	3.2696E-06
3.3000E+01*	7.5159E-06	5.2815E-06	2.6132E-06	7.1803E-07	6.8539E-07	2.3153E-06
3.5000E+01*	5.6924E-06	4.0465E-06	2.0998E-06	6.5581E-07	4.8679E-07	1.8085E-06
3.7000E+01*	4.4969E-06	3.2271E-06	1.6980E-06	5.8268E-07	4.3034E-07	1.5215E-06
3.9000E+01*	3.5848E-06	2.5957E-06	1.3980E-06	5.1420E-07	3.8571E-07	1.0073E-06
4.1000E+01*	2.8723E-06	2.0965E-06	1.1546E-06	4.5043E-07	3.1006E-07	8.4506E-07
4.3000E+01*	2.3854E-06	1.7559E-06	9.4627E-07	3.8907E-07	2.7103E-07	7.5126E-07
4.5000E+01*	1.9522E-06	1.4472E-06	8.2789E-07	3.2517E-07	2.3832E-07	5.0779E-07

TABLE VI

CYLINDRICAL GEOMETRY C= 3.0000E-01 SCALAR FLUX - ISOTROPIC SOURCE

POLE COMPARISON

T/X	1.0000E+00	2.0000E+00	3.0000E+00	4.0000E+00	5.0000E+00	6.0000E+00
1.0000E+00*	∞	0.	0.	0.	0.	0.
3.0000E+00*	2.9596E-02	2.7184E-02	∞	0.	0.	0.
5.0000E+00*	4.9675E-03	2.0126E-03	3.9452E-03	3.0123E-02	∞	0.
7.0000E+00*	3.4839E-04	6.3291E-04	1.2184E-03	3.9488E-04	3.9286E-03	2.2974E-02
9.0000E+00*	5.7703E-04	9.5634E-04	1.3633E-03	1.6092E-03	1.5248E-03	1.6551E-03
1.1000E+01*	6.5916E-04	9.0684E-04	1.1358E-03	1.3361E-03	1.5812E-03	2.0930E-03
1.3000E+01*	5.9335E-04	7.2810E-04	8.7539E-04	1.0278E-03	1.2295E-03	1.6006E-03
1.5000E+01*	5.0757E-04	5.7698E-04	6.6770E-04	7.8827E-04	9.4477E-04	1.1937E-03
1.7000E+01*	4.3045E-04	4.7656E-04	5.3727E-04	6.2094E-04	7.3573E-04	9.1265E-04
1.9000E+01*	3.6653E-04	3.9724E-04	4.4566E-04	5.0217E-04	5.8654E-04	7.1453E-04
2.1000E+01*	3.1459E-04	3.3634E-04	3.7020E-04	4.1500E-04	4.7843E-04	5.7088E-04
2.3000E+01*	2.7238E-04	2.8844E-04	3.1411E-04	3.4950E-04	3.9791E-04	4.6878E-04
2.5000E+01*	2.3832E-04	2.5012E-04	2.7006E-04	2.9803E-04	3.3613E-04	3.9163E-04
2.7000E+01*	2.0961E-04	2.1904E-04	2.3480E-04	2.5725E-04	2.8797E-04	3.3194E-04
2.9000E+01*	1.8573E-04	1.9336E-04	2.0610E-04	2.2437E-04	2.4951E-04	2.8493E-04
3.1000E+01*	1.6556E-04	1.7194E-04	1.8242E-04	1.9743E-04	2.1829E-04	2.4724E-04
3.3000E+01*	1.4861E-04	1.5384E-04	1.6263E-04	1.7505E-04	1.9258E-04	2.1656E-04
3.5000E+01*	1.3411E-04	1.3850E-04	1.4588E-04	1.5653E-04	1.7115E-04	1.9123E-04
3.7000E+01*	1.2162E-04	1.2534E-04	1.3162E-04	1.4069E-04	1.5310E-04	1.7007E-04
3.9000E+01*	1.1079E-04	1.1397E-04	1.1935E-04	1.2713E-04	1.3652E-04	1.5220E-04
4.1000E+01*	1.0135E-04	1.0408E-04	1.0872E-04	1.1544E-04	1.2466E-04	1.3694E-04
4.3000E+01*	9.2994E-05	9.5389E-05	9.9457E-05	1.0529E-04	1.1329E-04	1.2380E-04
4.5000E+01*	8.5673E-05	8.7767E-05	9.1346E-05	9.6417E-05	1.0338E-04	1.1275E-04

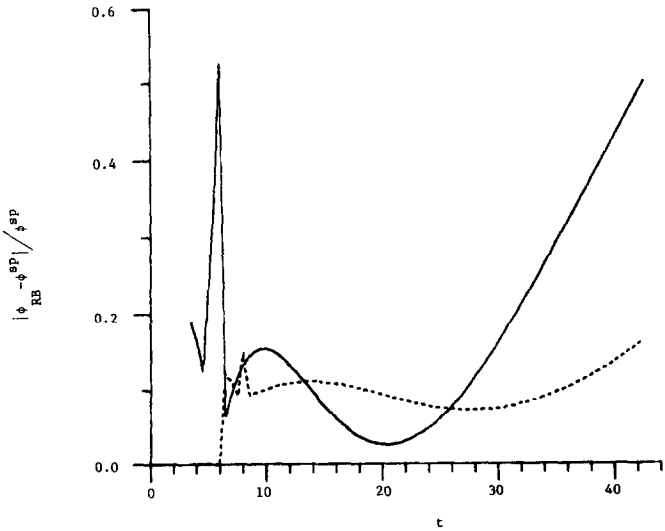

FIG. 1. Relative error in comparison with Ref. [1] (ϕ_{RB}) for positions $r = 3$(—) and 6(– – –) for $c = 0.3$.

The claim in Ref. [1] that the fitted solution is more accurate than either the TDA or Monte Carlo solutions is apparently not true.

The figure sequence Figs. 2a and b is a demonstration of the moment expansion for linearly anisotropic scattering

$$\omega_0 = 1$$

$$|\omega_1| \leqslant \tfrac{1}{3}; \qquad \omega_l = 0,\ l \geqslant 2$$

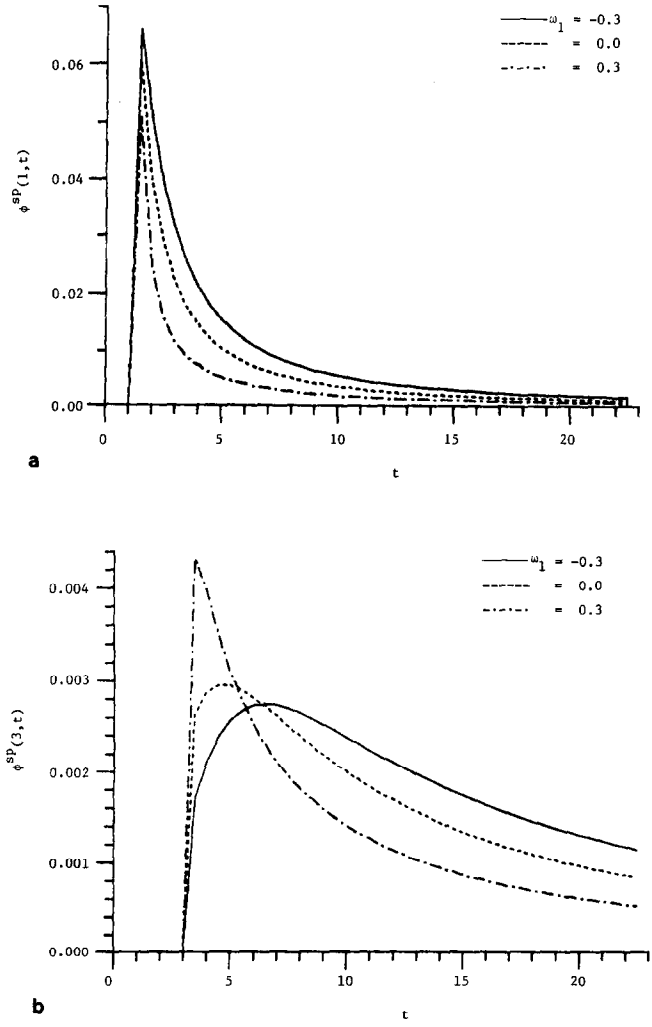

FIG. 2(a). Scalar flux in spherical geometry for linearly anisotropic scattering $r = 1$ and $c = 1$. (b) Scalar flux in spherical geometry for linearly anisotropic scattering for $r = 3$ and $c = 1$.

and $c = 1$. The restriction on ω_1 is required in order to retain the nonnegativity of the scattering differential cross section. To the author's knowledge, these results are the first semi-analytical results to appear in the literature where both time dependence and anisotropic scattering have been considered. Quantitatively, the results seem correct in that the less forward peaked the scattering cross section is the longer it takes for the bulk of the neutrons to pass a given spatial position. Tables VII and VIII give the relative error between the exact solution and diffusion theory with the transport corrected diffusion coefficient given by

$$D = \frac{1}{3c(1-\omega_1)}.$$

As required from theory, the exact solution still approaches diffusion theory with increasing time although at a slower rate than for the isotropic scattering case.

7. Conclusion

A new polynomial expansion for the solution of the time-dependent monoenergetic neutron transport equation in infinite geometry has been proposed and verified. The solution is represented as a summation over moments which can be determined in closed form thus allowing accurate numerical evaluation. The solution representation also allows generalization to anisotropic scattering by using moments determined from multiple collision theory. The solution does possess several shortcomings, however. Near a flux discontinuity (wavefront) many terms in the expansion are required for high (four places) accuracy. As a result, round off error accumulation eventually will render the solution very near the wavefront useless. This difficulty is inherent in any moments reconstruction algorithm since it is at best a marginally numerically stable technique where high quality information $[\phi(r, t)]$ is inferred from the lower quality information contained by the moments. Methods are currently being investigated to increase the stability of the reconstruction. In addition, a similar reconstruction has been developed for the angular flux in infinite plane geometry resulting from both a localized pulsed isotropic and beam source. A knowledge of the Greens function (beam source) will then allow the numerical evalution of solutions in finite geometry which will be the subject of a future article.

Appendix

V. C. Boffi, in a very comprehensive treatment of the time-dependent transport equation in plane geometry using transforms [6], evaluated the pole portion of the

TABLE VII

SPHERICAL GEOMETRY C= 1.0000E+00 SCALAR FLUX - ISOTROPIC SOURCE

ANISOTROPIC SCATTRERING ω_1 =-0.3

T/X	1.0000E+00	2.0000E+00	3.0000E+00	4.0000E+00	5.0000E+00
1.0000E+00*	∞	0.	0.	0.	0.
3.0000E+00*	2.2409E-01	3.9011E-02	∞	0.	0.
5.0000E+00*	1.6942E-01	9.6050E-02	4.3720E-02	3.1000E-01	∞
7.0000E+00*	1.3465E-01	9.4115E-02	2.2656E-02	8.9032E-02	2.6660E-01
9.0000E+00*	1.1144E-01	8.5547E-02	4.1182E-02	2.4213E-02	1.1638E-01
1.1000E+01*	9.4954E-02	7.6946E-02	4.6486E-02	2.7060E-03	5.6220E-02
1.3000E+01*	8.2682E-02	6.9420E-02	4.7136E-02	1.5516E-02	2.6116E-02
1.5000E+01*	7.3202E-02	6.3027E-02	4.5983E-02	2.1976E-02	9.2415E-03
1.7000E+01*	6.5663E-02	5.7602E-02	4.4136E-02	2.5237E-02	8.4210E-04
1.9000E+01*	5.9524E-02	5.2980E-02	4.2067E-02	2.6791E-02	7.1500E-03
2.1000E+01*	5.4434E-02	4.9014E-02	3.9989E-02	2.7372E-02	1.1191E-02
2.3000E+01*	5.0144E-02	4.5580E-02	3.7989E-02	2.7388E-02	1.3780E-02
2.5000E+01*	4.6476E-02	4.2584E-02	3.6125E-02	2.7073E-02	1.5496E-02
2.7000E+01*	4.3311E-02	3.9948E-02	3.4391E-02	2.6565E-02	1.6589E-02
2.9000E+01*	4.0549E-02	3.7615E-02	3.2787E-02	2.5946E-02	1.7258E-02
3.1000E+01*	3.8114E-02	3.5533E-02	3.1274E-02	2.5273E-02	1.7632E-02
3.3000E+01*	3.5958E-02	3.3669E-02	2.9884E-02	2.4571E-02	1.7799E-02
3.5000E+01*	3.4029E-02	3.1985E-02	2.8614E-02	2.3869E-02	1.7823E-02
3.7000E+01*	3.2300E-02	3.0464E-02	2.7428E-02	2.3178E-02	1.7744E-02
3.9000E+01*	3.0734E-02	2.9075E-02	2.6333E-02	2.2506E-02	1.7589E-02
4.1000E+01*	2.9317E-02	2.7811E-02	2.5321E-02	2.1858E-02	1.7387E-02
4.3000E+01*	2.8020E-02	2.6646E-02	2.4377E-02	2.1236E-02	1.7144E-02

TABLE VIII

SPHERICAL GEOMETRY C= 1.0000E+00 SCALAR FLUX - ISOTROPIC SOURCE

ANISOTROPIC SCATTRERING ω_1 =+0.3

T/X	1.0000E+00	2.0000E+00	3.0000E+00	4.0000E+00	5.0000E+00
1.0000E+00*	∞	0.	0.	0.	0.
3.0000E+00*	2.8730E-02	3.6778E-01	∞	0.	0.
5.0000E+00*	3.4504E-02	9.8090E-02	2.3794E-01	2.3211E-01	∞
7.0000E+00*	3.1124E-02	3.1396E-02	1.1243E-01	1.7506E-01	1.4512E-01
9.0000E+00*	2.4904E-02	1.1218E-02	6.1168E-02	1.0961E-01	1.3223E-01
1.1000E+01*	2.0283E-02	3.3224E-03	3.7139E-02	7.3026E-02	9.9125E-02
1.3000E+01*	1.7019E-02	3.4455E-04	2.4121E-02	5.1485E-02	7.4834E-02
1.5000E+01*	1.4647E-02	2.2263E-03	1.6320E-02	3.7816E-02	5.7823E-02
1.7000E+01*	1.2858E-02	3.2410E-03	1.1312E-02	2.8622E-02	4.5658E-02
1.9000E+01*	1.1461E-02	3.7935E-03	7.9336E-03	2.2161E-02	3.6722E-02
2.1000E+01*	1.0342E-02	4.0834E-03	5.5696E-03	1.7463E-02	2.9996E-02
2.3000E+01*	9.4230E-03	4.2183E-03	3.8665E-03	1.3954E-02	2.4825E-02
2.5000E+01*	8.6557E-03	4.2584E-03	2.6118E-03	1.1273E-02	2.0775E-02
2.7000E+01*	8.0045E-03	4.2407E-03	1.6696E-03	9.1861E-03	1.7552E-02
2.9000E+01*	7.4453E-03	4.1866E-03	9.5163E-04	7.5368E-03	1.4952E-02
3.1000E+01*	6.9592E-03	4.1110E-03	3.9761E-04	6.2101E-03	1.2826E-02
3.3000E+01*	6.5332E-03	4.0218E-03	3.4374E-05	5.1363E-03	1.1075E-02
3.5000E+01*	6.1570E-03	3.9260E-03	3.7364E-04	4.2532E-03	9.6085E-03
3.7000E+01*	5.8209E-03	3.8262E-03	6.4223E-04	3.5239E-03	8.3784E-03
3.9000E+01*	5.5206E-03	3.7262E-03	8.5531E-04	2.9139E-03	7.3530E-03
4.1000E+01*	5.2503E-03	3.6274E-03	1.0255E-03	2.4019E-03	6.4480E-03
4.3000E+01*	5.0037E-03	3.5293E-03	1.1617E-03	1.9682E-03	5.6855E-03
4.3000E+01*	5.0037E-03	3.5293E-03	1.1617E-03	1.9682E-03	5.6855E-03

TABLE A

$a_1 = 0.35$	$a_8 = 0.075804$
$a_2 = 0.099107$	$a_9 = 0.017411$
$a_3 = 0.1$	$a_{10} = 0.032305$
$a_4 = 0.027723$	$a_{11} = 0.008075$
$a_5 = 0.010714$	$a_{12} = 0.001395$
$a_6 = 0.0125$	$a_{14} = 0.000357$
$a_7 = 0.031141$	

transport solution, representing the long time behavior, to a high degree of accuracy

$$\phi^{\mathrm{pl}}(x, t) = e^{-(1-c)t} \frac{e^{-x^2/4Dt}}{(4\pi Dt)^{1/2}} \xi(x, t)$$

where

$$\begin{aligned}
\xi(x, t) &= 1 + a_1/ct \\
&+ [a_2 - a_3(cx\sqrt{3})^2] \frac{1}{(ct)^2} - [a_4 - a_5(cx\sqrt{3})^2] \\
&+ [a_6(cx\sqrt{3})^4] \frac{1}{(ct)^3} + [-a_7 + a_8(cx\sqrt{3})^2 - a_9(cx\sqrt{3})^4] \frac{1}{(ct)^4} \\
&- [-a_{10} + a_{11}(cx\sqrt{3})^2 + a_{12}(cx\sqrt{3})^4 + a_{14}(cx\sqrt{3})^6] \frac{1}{(ct)^5} \\
&+ O((ct)^{-6}).
\end{aligned}$$

The values of the constants a_i are given in Table A. Then applying the geometrical tranformations given by Eqs. (2) and (13) gives:

$$\phi^{\mathrm{sp}}(r, t) = \frac{e^{-(1-c)t}}{(4\pi Dt)^{3/2}} e^{-r^2/4Dt} \left[\xi - \frac{2Dt}{r} \frac{d\xi}{dr} \right]$$

$$\begin{aligned}
\phi^{\mathrm{cy}}(r, t) = \frac{e^{-(1-c)t}}{4\pi Dt} e^{-r^2/4Dt} [&\{1 + a_1/ct + a_2/(ct)^2 \\
&- a_4/(ct)^3 - a_7/(ct)^4 + a_{10}/(ct)^5 + 3c^2[-a_3/(ct)^2 + a_5/(ct)^3 \\
&- a_8/(ct)^4 - a_{11}/(ct)^5] I_1 - 9c^4[a_6/(ct)^3 + a_9/(ct)^4 \\
&+ a_{12}/(ct)^5] I_2 - 27c^6[a_{14}/(ct)^5] I_3\} + 2Dt\{3c^2[-a_3/(ct)^2 \\
&+ a_5/(ct)^3 + a_8/(ct)^4 - a_{11}/(ct)^5] - 36c^4[a_6/(ct)^3 \\
&+ a_9/(ct)^4 + a_{12}/(ct)^5] I_1 - 162c^6[a_{14}/(ct)^5] I_2\}]
\end{aligned}$$

$$I_0 = e^{-r^2/4Dt}\sqrt{4\pi\, Dt}$$

$$I_1 = I_0[r^2 + 2Dt]$$

$$I_2 = I_0[r^4 + 4\pi\, Dr^2 t + 12D^2t^2]$$

$$I_3 = I_0[r^6 + 6Dtr^4 + 36D^2t^2r^2 + 120D^3t^3].$$

REFERENCES

1. J. H. RENKEN AND F. BIGGS, *J. Comput. Phys.* **9** (1972), 318.
2. K. M. CASE AND P. F. ZWEIFEL, "Linear Transport Theory," Addison–Wesley, Reading, Mass., 1967.
3. B. D. GANAPOL, P. W. MCKENTY, AND K. L. PEDDICORD, *Nucl. Sci. Eng.* **64** (1977), 317.
4. N. N. LEBEDEV, "Special Functions and Their Applications," Prentice–Hall, Englewood Cliffs, N.J., 1965.
5. B. D. GANAPOL, *Nucl. Sci. Eng.* **89** (1985), 256.
6. V. C. BOFFI, *Nukleonik* **8** (1966), 448.